Energy Storage Materials 13 (2018) 80–87

Contents lists available at ScienceDirect

Energy Storage Materials

journal homepage: www.elsevier.com/locate/ensm

Two-dimensional boron as an impressive lithium-sulphur battery cathode material

Sean Grixti[a], Sankha Mukherjee[a], Chandra Veer Singh[a,b,*]

[a] Department of Materials Science and Engineering, University of Toronto, Toronto, Ontario, Canada M5S 3E4
[b] Department of Mechanical and Industrial Engineering, University of Toronto, Ontario, Canada M5S 3G8

ABSTRACT

β_{12}-borophene is a recently fabricated two-dimensional (2D) allotrope of boron that has many unique electrical, mechanical and chemical properties that make it an excellent candidate as a cathode material in lithium sulphur (Li-S) batteries. Ab initio calculations were performed to determine β_{12}-borophene's applicability as a Li-S battery cathode material. Binding energies of sulphur (S_8) and various lithium polysulphides (Li_2S_x, x=2,3,4,6,8) on the β_{12}-borophene surface were calculated, along with the diffusion barriers for Li_2S_6 and Li_2S_4. Our calculations suggest a moderate adsorption of sulphur and a strong adsorption of all lithium polysulphides, implying β_{12}-borophene would sufficiently inhibit the dissolution of lithium polysulphides into the electrolyte, preventing the "shuttle effect". Through an exhaustive adsorption site sampling the binding energies were determined to be −1.19 eV for S_8, −2.98 eV for Li_2S_8, −2.77 eV for Li_2S_6, −3.08 eV for Li_2S_4, −3.48 eV for Li_2S_3, −3.79 eV for Li_2S_2, and −4.57 eV for Li_2S. The diffusion barriers for Li_2S_6 and Li_2S_4 were determined to be moderate, ensuring efficient diffusion, with the lowest diffusion energy barriers being 0.61 eV and 0.99 eV for Li_2S_6 and Li_2S_4, respectively. The strong binding energies and moderate diffusion barriers suggest β_{12}-borophene would be an excellent lithium polysulphide immobilizer in Li-S cathodes.

1. Introduction

With the recent boom in the electric vehicle market and the need for grid level energy storage, the demand for cheaper, safer, and more energy dense batteries is greater than ever [1,2]. The lithium sulphur (Li-S) battery is a rechargeable battery made primarily from lithium and sulphur; it is inherently safer than Li-ion, more environmentally friendly, and possesses a higher theoretical energy density [2–7]. A two-electron redox site provided by sulphur, coupled with the high capacity of the Li-metal anode gives Li-S batteries a staggering theoretical specific capacity of 1672 mA h g^{-1} and a theoretical energy density of 2600 W h kg^{-1} [6,7]. During discharge lithium dissociates from the anode, into an electrolyte medium, and then undergoes an electrochemical reaction with elemental sulphur at the cathode to produce Li_2S. During the formation of the final Li_2S product multiple lithium polysulphides, Li_2S_x (x=2,3,4,6,8), are produced [3,6].

Large scale commercial use of Li-S batteries has yet to be seen due to technical obstacles causing low coulombic efficiencies, permanent capacity losses and short cycle lives. These technical issues mainly stem from the construction of the sulphur cathode. Elemental sulphur and Li_2S are both insulators, so a conductive material additive is required to provide a conductive path through the electrode. In small scale commercial Li-S batteries carbon is added to the cathode to provide a conductive path; however, another issue occurs during discharge [38]. During discharge, the lithium polysulphides that are formed have a tendency to dissolve into the electrolyte solution, deposit onto the anode and create a passivation layer, preventing the redeposition of lithium during charging. This issue is known as the "shuttle effect", and is the main cause of short cycle lives and capacity loss [2–7]. To mitigate these issues, a conductive material that also sufficiently adsorbs the lithium polysulfides is needed as an additive to replace or compliment the carbon in the sulphur cathodes.

With the recent advancements in synthetic methods, high theoretical surface areas, and unique electronic properties, nanostructued two-dimensional (2D) materials appear to be emerging as an ideal candidate for Li-S cathode materials [8]. Many nanostructured carbon materials such as nanoporous carbon, graphene, doped graphene and graphene oxide, have already shown promise theoretically and experimentally as potential Li_2S_x anchor materials [9–12,39,42,45,46]. Other 2D structures, such as transition metal oxides, sulfides and chlorides, and phosphorene have also displayed their ability to sufficiently immobilize the lithium polysulphide species [13–17,43,44]. One

---

[*] Corresponding author at: Department of Materials Science and Engineering, University of Toronto, Toronto, Ontario, Canada M5S 3E4.
E-mail address: chandraveer.singh@utoronto.ca (C.V. Singh).

https://doi.org/10.1016/j.ensm.2017.12.024
Received 10 November 2017; Received in revised form 20 December 2017; Accepted 23 December 2017

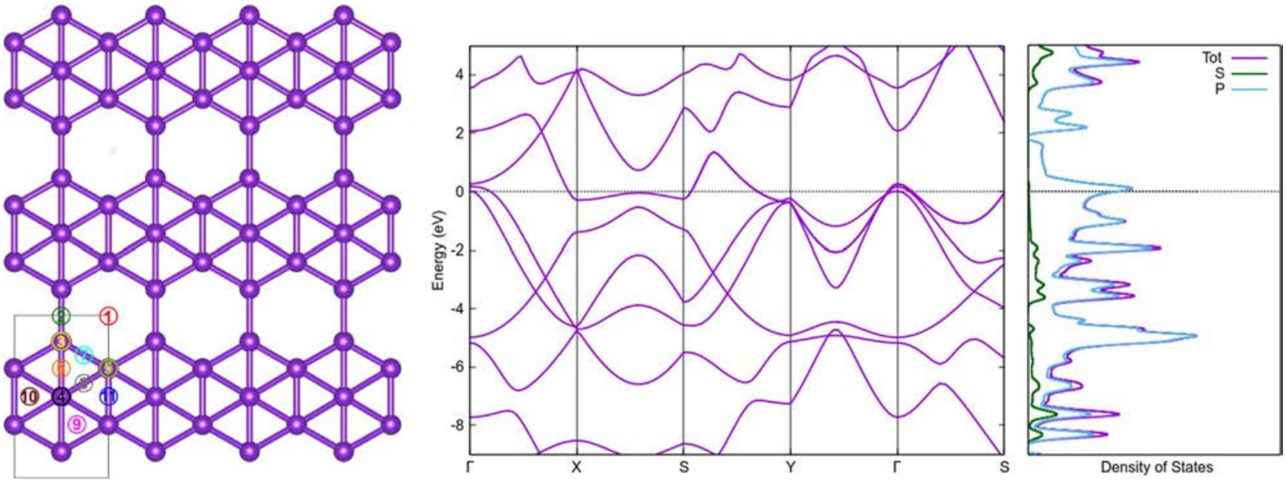

Fig. 1. *Left* The β_{12}-borophene 4×3 supercell structure, with the irreducible unit cell shown by the black rectangle, the 11 symmetrically distinct binding sites shown in red. *Right* Band structure and projected density of states shown.

potential candidate for Li_2S_x immobilization in Li-S batteries is borophene.

Borophene is a recently fabricated 2D allotrope of boron that has been synthesized as three different allotropes on Ag(111) substrates [26–29]. The β_{12}-borophene allotrope has proven to be an extraordinary anode material in Li-ion and Na-ion batteries, and is therefore a promising candidate as an anchor material in the cathodes of Li-S batteries [18–20]. β_{12}-borophene is an intriguing 2D material as it is intrinsically metallic, giving it a high electrical conductivity [21,22]. It possesses a high stiffness, tensile strength and chemical stability making it suitable for the harsh environments present in batteries [23–25]. β_{12}-borophene's performance as Li-ion and Na-ion battery anodes, and unique properties suggests it is the best place to start for an inquiry into the application of borophene in Li-S battery cathodes [26–29]. To investigate β_{12}-borophene's potential as a Li-S battery cathode material, ab initio simulations were performed to determine the adsorption energies of the Li_2S_x compounds on the β_{12}-borophene surface and the barriers associated with their diffusion.

2. Computational details

First principles calculations are performed based on the density functional theory (DFT) framework, as implemented in the Quantum Espresso (QE) suite [30]. The generalized gradient approximation (GGA) with the Perdew-Burke-Ernzerhof (PBE) functional was used for the exchange-correlation [31]. Vanderbuilt pseudopotentials were utilized to perform geometric relaxation and electronic structure calculations, while PAW pseudopotentials were utilized for Bader charge analysis calculations. The cut-off energy for the plane-wave expansion was set to 60 Ry. To accurately describe the 2D structure and eliminate any artificial interlayer interactions a vacuum space of 20 Å was used. Both the atomic positions and the lattice constant were relaxed using a convergence threshold of 10^{-6} eV for energy and 10^{-3} eV Å^{-1} for force. A Monkhorst-Pack k-point mesh was used with sizes of 13 × 13 × 3 for the geometrical relaxation, 4 × 4 × 1 for the adsorption calculations, and 20 × 20 × 1 for the electronic structure calculations [32]. The DFT-D2 method was used to take into account the long-range Van der Waals interactions [33]. The activation energy barriers for the diffusion of Li_2S_x across the borophene surface was calculated using the climbing image nudged elastic band (CI-NEB) method, where images along the minimum energy pathway (MEP) are created between designated initial and final atomic positions [34]. A 4 × 3 supercell was used as the surface for the binding energy and CI-NEB calculations.

The adsorption energies (E_{ads}) were calculated using the following equation:

$$E_{ads} = E_{B+Li_2S_x} - E_B - E_{Li_2S_x} \tag{1}$$

where $E_{B+Li2Sx}$ is the energy of β_{12}-borophene after the adsorption of the Li_2S_x species of interest, E_B is the energy of the free standing β_{12}-borophene supercell, and E_{Li2Sx} is the energy of the free standing Li_2S_x species of interest. Negative values for E_{ads} are indicative of a spontaneous adsorption, and indicate the binding energy.

Charge density difference calculations were performed to gather insight into the electronic interactions between the Li_2S_x species and the β_{12}-borophene surface. The charge density difference ($\Delta\rho_{ads}$) for each system was calculated using the following equation:

$$\Delta\rho_{ads} = \rho_{B+Li_2S_x} - \rho_{Li_2S_x} - \rho_B \tag{2}$$

Where $\rho_{B+Li2Sx}$ is the charge density of β_{12}-borophene after adsorption of the Li_2S_x species of interest, ρ_B is the charge density of free standing β_{12}-borophene, and $\rho_{L:i2Sx}$ is the charge density of the free standing Li_2S_x species of interest.

3. Results and discussion

3.1. *Crystal structure of β_{12}-borophene*

The relaxed structure of β_{12}-borophene can be seen Fig. 1. The lattice parameters of the unit cell were determined to be a=2.92621 Å and b=5.06337 Å, giving good agreement with previously calculated and experimentally determined lattice parameters of a=2.926 Å and b=5.068 Å, and a=3 Å and b=5 Å, respectively [18,29]. The structure is very unique, having a significant concentration of vacancies, with the vacancy sites occurring in periodic rows.

3.2. *Adsorption of Li_2S_x on the β_{12}-borophene surface*

A comprehensive adsorption site sampling for each Li_2S_x species and S_8 was performed. Each compound was tested at the 11 symmetrically unique sites on the β_{12}-borophene's surface, as seen in Fig. 1, and at two different rotational orientations to obtain the most stable adsorption site. The various orientations and positions tested can be seen in Fig. 2. The binding energies at each orientation and position vary, as seen in Fig. 2 and Fig. S1, but through the meticulous adsorption site sampling the most stable site was determined for S_8 and each Li_2S_x species. The most stable S_8 and Li_2S_x configurations on the β_{12}-borophene surface can be seen in Fig. 3. S_8 and each Li_2S_x species binds strongly to the β_{12}-borophene surface, with the strongest

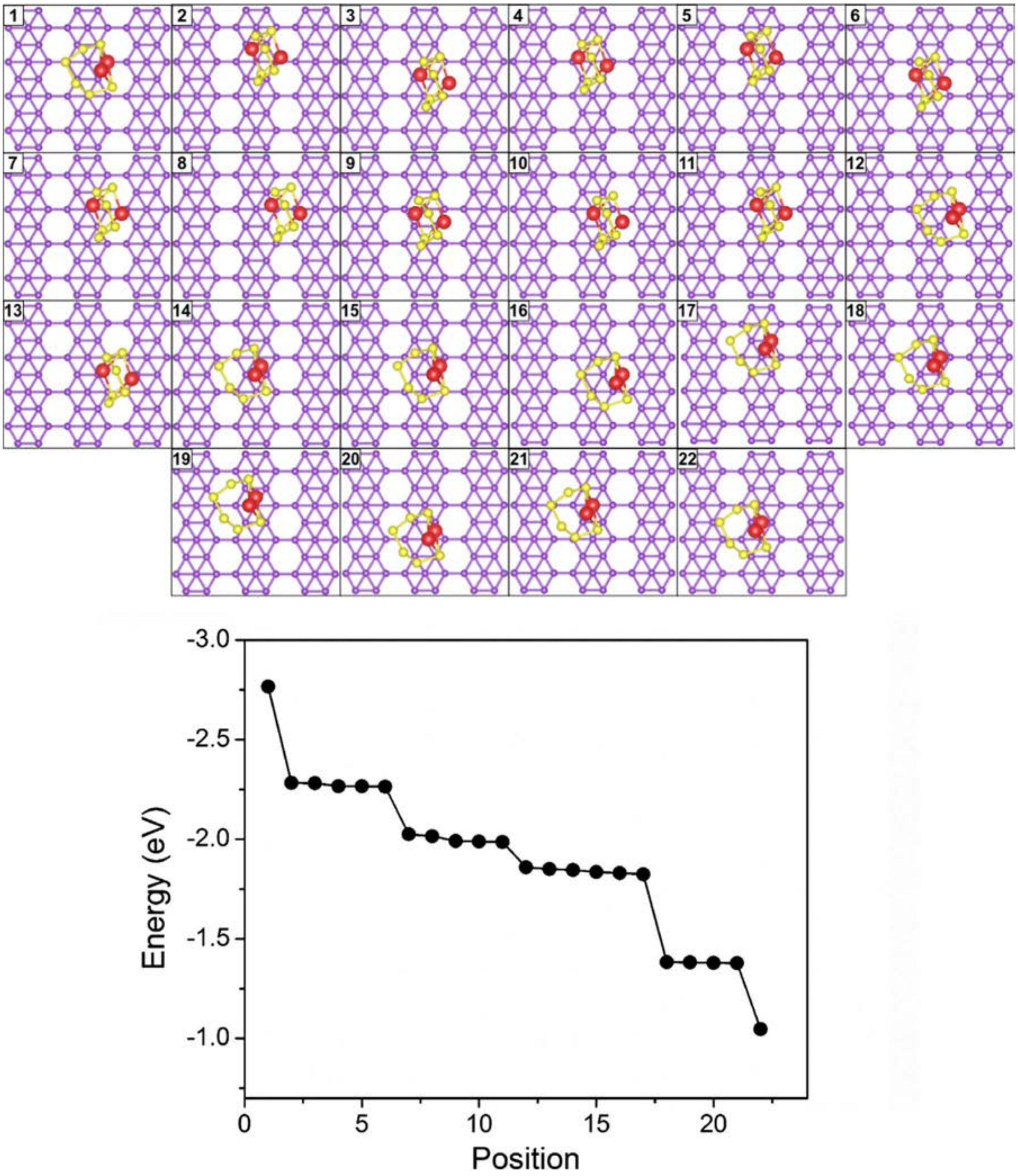

Fig. 2. *Top)* View of initial Li_2S_6 positions at all tested sites. *Bottom)* Binding energy of Li_2S_6 on the β_{12}-borophene surface at each site.

binding energy for each compound being: −1.19 eV for S_8, −2.98 eV for Li_2S_8, −2.77 eV for Li_2S_6, −3.08 eV for Li_2S_4, −3.48 eV for Li_2S_3, −3.79 eV for Li_2S_2, and −4.57 eV for Li_2S, as seen in Table 1. These large binding energies coincide with previous findings of boron's role as a lithium polysulphide immobilizer, where boron doping of graphene was found to increase the binding strength of various Li_2S_x species [40]. These binding energies are smaller than single vacancy graphene, which has binding energies for large lithium polysulphides (Li_2S_8, Li_2S_6 and Li_2S_4) as strong as −4.64 eV [10]. Contrarily, the binding strength of β_{12}-borophene is significantly stronger than other previously studied 2D materials, such as phosphorene and monolayer ReS_2, which achieve binding energies as strong as −2.5 eV and −2.66 eV, respectively [16,35]. It is noted that there is a general trend of increasing binding strength with the decreasing lithium polysulphide size, and it is also noted that all Li_2S_x species have significantly stronger binding energies when compared to S_8. The binding energy of S_8 is significantly lower than the Li_2S_x species due to the lack of lithium participating in bonding. The moderate binding energy of S_8, and increasing binding strength with decreasing Li_2S_x size assures that the formation of Li_2S on the β_{12}-borophene surface is still spontaneous.

It has previously been suggested that binding energies stronger than −2 eV could produce significant distortion to the lithium polysulphide structure, preventing it from participating in the subsequent reactions [15]. However, structural deformation is only observed for the large lithium polysulphides (Li_2S_8 and Li_2S_6), when bound to the β_{12}-borophene surface, as seen in Fig. 3. When compared to other theoretically and experimentally investigated 2D Li_2S_x immobilizers, such as titanium based MXenes, less structural deformation is observed on β_{12}-borophene, at comparable binding energies [41,47]. It is also noted that these lithium polysulfides have high internal degrees of freedom, making them more susceptible to entropic effects, which are not taken into account at 0 K DFT calculations. Entropic effects should

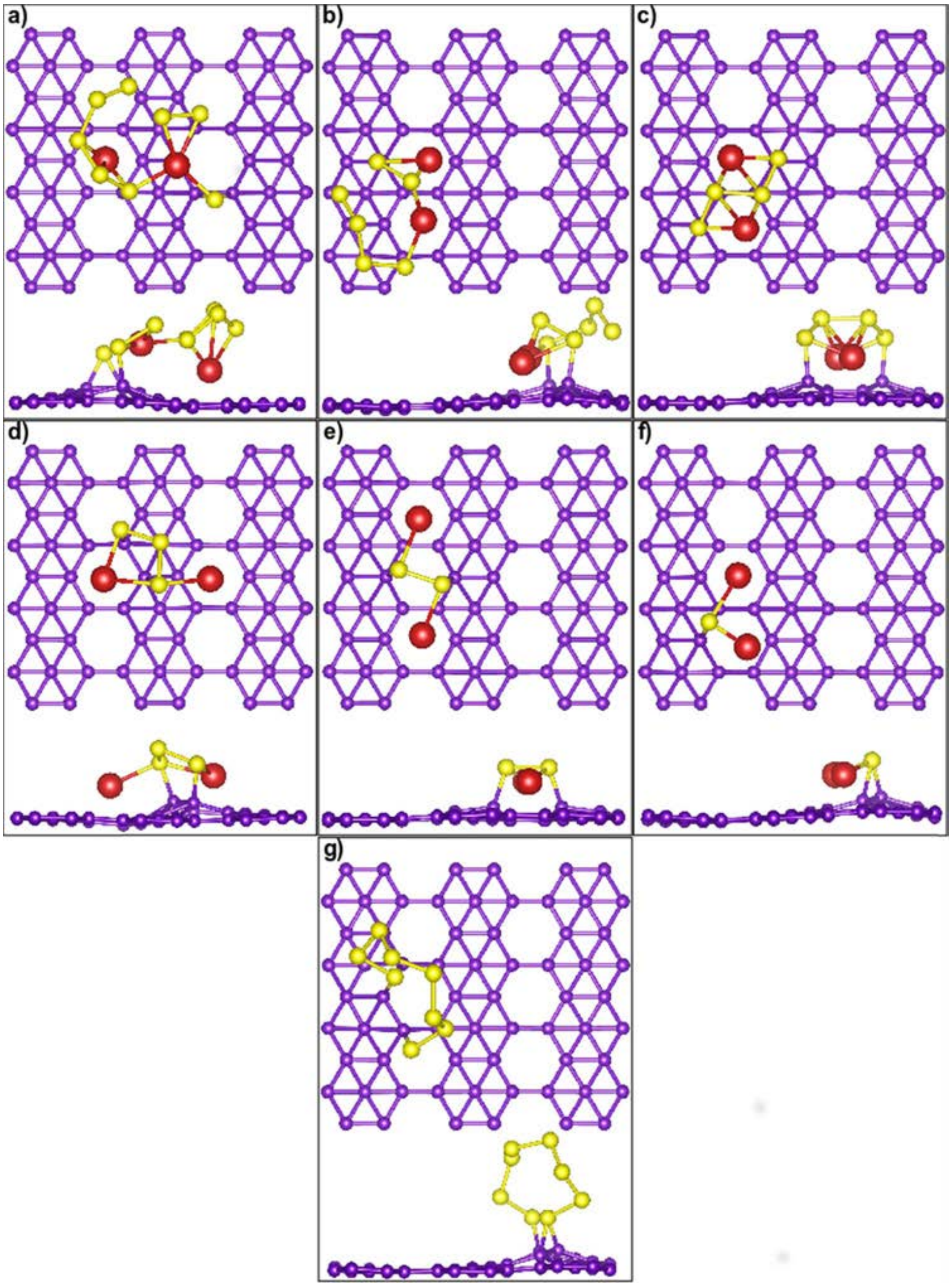

Fig. 3. Top and side view of bound (a) Li_2S_8 (b) Li_2S_6 (c) Li_2S_4 d) Li_2S_3 (e) Li_2S_2 (f) Li_2S, and (g) S_8 systems.

Table 1
Binding energies and corresponding shortest distance of Li_2S_x compounds on the β_{12}-borophene surface.

	Li_2S_8	Li_2S_6	Li_2S_4	Li_2S_3	Li_2S_2	Li_2S	S_8
Binding Energy (eV)	−2.98	−2.77	−3.08	−3.48	−3.79	−4.57	−1.19
d $_{Li2Sx-B}$ (Å)	1.77	1.93	2.02	1.85	1.87	1.73	1.91

therefore decrease the binding strength of each Li_2S_x species, suggesting these strong binding energies are preferential as they will be more stable at operating conditions.

It is observed that in all Li_2S_x systems the lithium atoms sit above the β_{12}-borophene's intrinsic vacancies. This is due to the difference in electronegativity between boron and lithium, as the "dangling bonds" of the boron atoms on the edge of the intrinsic vacancies can facilitate the greatest electron transfer, as seen in Fig. 4. All of the Li_2S_x species bind very closely to the β_{12}-borophene surface, with Li_2S binding the closest with a distance of 1.73 Å, as seen in Table 1. These very close binding distances coincide with the strong binding energies. From the charge density plots, seen in Fig. 4 and Fig. S2, and the Bader charge analysis, seen in Table 2, it is evident that both lithium and sulphur actively participate in bonding with the β_{12}-borophene surface. The lithium-borophene bonding is characterized with electron transfer from the lithium atom to the β_{12}-borophene surface, due to the difference in electronegativity of lithium and boron. The sulphur-borophene bonding is characterized by electron transfer from the β_{12}-borophene surface to the sulphur atoms, due to the difference in electronegativity of sulphur and boron. The active participation of both lithium and sulphur when binding to the β_{12}-borophene surface creates a constructive bonding character creating the large binding energies seen in Table 1. It is noted that there is an overall charge gain for Li_2S_8 when bound to the β_{12}-borophene surface, while there is an overall charge loss for the rest of the Li_2S_x species when bound to the β_{12}-

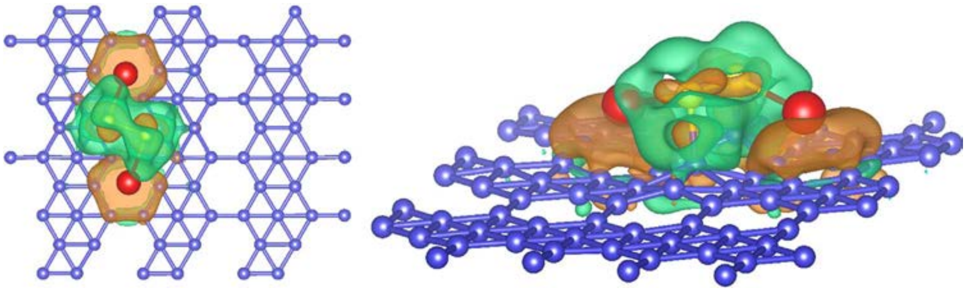

Fig. 4. Example differential charge density (DCD) between Li_2S_2, the β_{12}-borophene surface, and the bound system, with top and perspective views. The orange represents the spatial region of charge gain, and the green represents the spatial region of charge loss.

Table 2
Bader charge analysis of each Li_2S_x species, with average electronic charge gain for S and Li shown.

	Li_2S_8	Li_2S_6	Li_2S_4	Li_2S_3	Li_2S_2	Li_2S
Q_{Savg} (e^-)	0.33	0.21	0.33	0.46	0.66	0.94
Q_{Liavg} (e^-)	−0.87	−0.87	−0.87	−0.88	−0.89	−0.89
Q_{Li2Sx} (e^-)	0.89	−0.45	−0.40	−0.39	−0.45	−0.83

borophene surface, as seen in Table 2. This charge gain in Li_2S_8 can be explained by the high sulphur concentration in the Li_2S_8 species, coupled with some sulphur backbone decomposition on the β_{12}-borophene surface.

3.3. Electronic characteristics of β_{12}-borophene with bound Li_2S_x species

β_{12}-borophene is an ideal Li-S battery cathode material candidate due to its high electrical conductivity. To ensure β_{12}-borophene is still conductive after adsorption, projected density of states (PDOS) calculations were performed on the bound system for each Li_2S_x species. The PDOS plots of Li_2S_8, Li_2S_4, and Li_2S_2 can be seen in Fig. 5, as examples of long, medium and short chain lithium polysulphides, and the PDOS plots of Li_2S_6, Li_2S_3 and Li_2S can be seen in Fig. S3. All Li_2S_x bound systems have significant density of states at the fermi energy, meaning β_{12}-borophene remains metallic after adsorption, and therefore conductive. From the PDOS plots the bonding character of the lithium polysulphide chains and the β_{12}-borophene surface can be determined. There is a very small contribution of electron states from lithium in all systems, signifying the bonding character between the lithium atoms and the β_{12}-borophene surface is mostly ionic. This ionic interaction is corroborated by the Bader charge analysis of an average electron transfer of 0.87–0.89 electrons from Li to the β_{12}-borophene substrate in each system, as seen in Table 2.

Sulphur's contribution of electron states varies with lithium polysulphide size. In the Li_2S_8 bound system substantial electron states come from sulphur, and from the PDOS plot significant overlap in states between the sulphur 3p orbitals and boron 2p orbitals is observed, signifying a covalent bonding character between sulphur and the β_{12}-borophene surface. As the lithium polysulphide chain size decreases sulphur contributes less electron states, which can be explained by the decrease in sulphur concentration. The overlap between sulphur 3p states and boron 2p states is still observed, signifying the bonding character is still covalent. However, in Fig. S3 (c) minimal sulphur states are observed, with no hybridization occurring, signifying a more ionic bonding character. This ionic bonding character is corroborated with the Bader charge analysis, with sulphur gaining 0.94 electrons from the β_{12}-borophene substrate, as seen in Table 2.

3.4. Diffusion of Li_2S_x species across β_{12}-borophene

During the discharge of a Li-S battery rapid diffusion into the cathode is required to obtain maximal capacity, therefore the diffusion

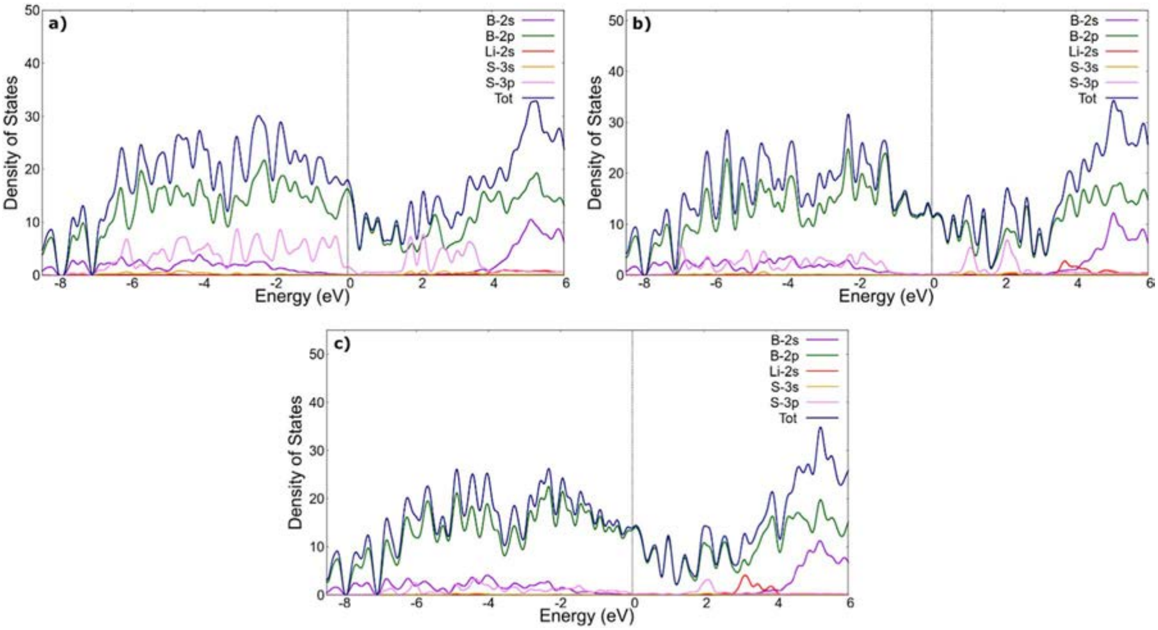

Fig. 5. Projected density of states of (a) Li_2S_8 (b) Li_2S_4 (c) Li_2S_2 bound systems, as examples of long, medium and short chained lithium polysulphides.

Table 3
Computed diffusion energy barriers across the x and y directions of the β_{12}-borophene surface.

Lithium Polysulfide Species	Diffusion Energy Barrier (eV)	
	Zigzag	Armchair
Li_2S_4	1.13	0.99
Li_2S_6	1.18	0.61

of the larger lithium polysulfides across the β_{12}-borophene surface needs to be quantified. The diffusion coefficient is proportional to the activation energy barrier through the Arrhenius equation:

$$D \propto e^{\frac{-E_a}{k_b T}} \tag{3}$$

where E_a is the activation energy required for the diffusion, k_b is the Boltzmann constant, and T is temperature. NEB calculations were performed to determine the energy barriers associated with diffusion of the most abundant large lithium polysulphides present during discharge, Li_2S_6 and Li_2S_4, across the β_{12}-borophene surface [36,37]. The diffusion was tested in both the x and y direction starting from the strongest binding site for each Li_2S_x species. The calculated barriers can be seen in Table 3 and Fig. 6.

The diffusion barriers in the zigzag direction of the Li_2S_x species are 1.13, and 1.18 for Li_2S_4, and Li_2S_6, respectively. In both Li_2S_x species the armchair direction had the lower diffusion energy barriers, with diffusion barriers of 0.99, and 0.61 eV for the Li_2S_4, and Li_2S_6 respectively. The minimum diffusion energy barriers are lower than some other nanostructured materials such as TiO_2/TiN decorated graphene, which has a diffusion barrier as low as 1.04 eV for Li_2S_4 [39]. However, they are still not as low as the diffusion barriers on black phosphorene, which has a minimum diffusion energy barrier of 0.28 eV and 0.19 eV for Li_2S_4 and Li_2S_6, respectively [16]. Interestingly, the lowest diffusion energy barrier of Li_2S_6 is comparable to that of Li ions across the β_{12}-borophene surface, with the minimum diffusion energy barrier of a Li ion across the β_{12}-borophene surface being 0.66 eV [18]. It is also noted that the preferred diffusion direction of a Li ion has previously been determined to be the zigzag direction, while the lithium polysulphides are found to prefer the armchair direction [18]. This difference in preferred diffusion paths shows the sulphur-borophene interaction plays a major role. These moderate diffusion energy barriers will allow for efficient transport of Li_2S_6 and Li_2S_4 into the cathode, and at operating temperatures diffusion barriers may be even lower due to lower binding energies.

4. Conclusions

In summary, β_{12}-borophene was investigated as a potential lithium polysulphide immobilizer for Li-S battery cathodes. By exhaustive adsorption site sampling the strongest binding energies for S_8, Li_2S_8, Li_2S_6, Li_2S_4, Li_2S_3, Li_2S_2 and Li_2S species were determined to be −1.19, −2.98, −.77, −3.08, −3.48, −3.79 and −4.57 eV, respectively. The binding energies of the Li_2S_x species on the β_{12}-borophene surface are quite strong; however, structural distortion is only seen in Li_2S_8 and Li_2S_6. Therefore, β_{12}-borophene may sufficiently prevent the dissolution of the Li_2S_x species into the electrolyte. After adsorption of S_8 and the Li_2S_x chains the metallic character of β_{12}-borophene is preserved, maintaining the ideal electronic properties needed as an electrode material. The smallest diffusion barriers associated with the diffusion of Li_2S_4, and Li2S$_6$ across the β_{12}-borophene surface were determined to be 0.99 and 0.61 eV, respectively. The strong binding

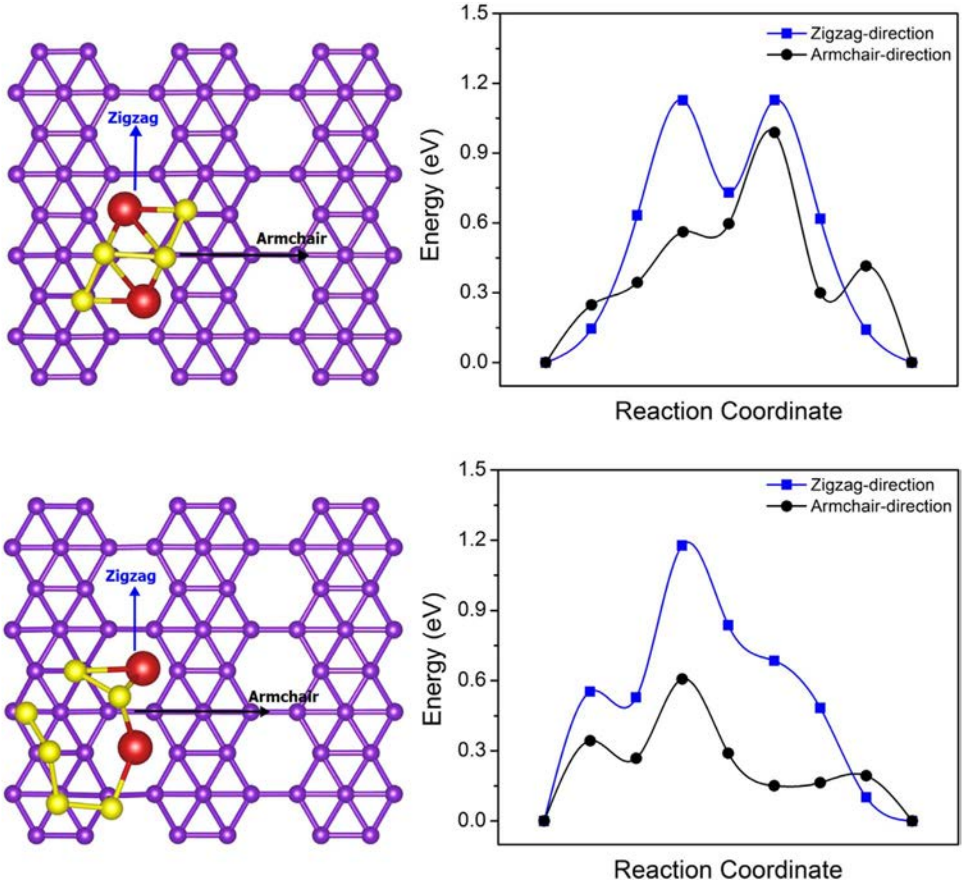

Fig. 6. Energy profile associated with the diffusion of Li_2S_4, and Li_2S_6, across the β_{12}-borophene surface in both the zigzag and armchair directions, starting from the determined strongest binding site, and ending at a symmetrically equivalent site.

energies and moderate diffusion energy barriers, as determined through the presented method, suggest β_{12}-borophene would be an excellent lithium polysulphide immobilizer in Li-S battery cathodes to prevent the dissolution of lithium polysulphides. In future works, other borophene allotropes should be investigated, as the staunch differences in atomic and electronic structures may also provide favourable electrode properties.

Acknowledgments

The authors acknowledge funding by the Natural Sciences and Engineering Research Council of Canada (NSERC) through the Discovery grant, the Hart Professorship, and the University of Toronto. We also acknowledge Compute Canada for providing computing resources at the SciNet, CalculQuebec, and Westgrid consortia.

Appendix A. Supporting information

Supplementary data associated with this article can be found in the online version at doi:10.1016/j.ensm.2017.12.024.

References

[1] J.B. Goodenough, A. Manthiram, A perspective on electrical energy storage, MRS Commun. 4 (2014) 135–142. http://dx.doi.org/10.1557/mrc.2014.36.
[2] A. Manthiram, Y. Fu, S.H. Chung, C. Zu, Y.S. Su, Rechargeable lithium-sulfur batteries, Chem. Rev. 114 (2014) 11751–11787. http://dx.doi.org/10.1021/cr500062v.
[3] D. Bresser, S. Passerini, B. Scrosati, Recent progress and remaining challenges in sulfur-based lithium secondary batteries – a review, Chem. Commun. 49 (2013) 10545. http://dx.doi.org/10.1039/c3cc46131a.
[4] J.R. Dahn, E.W. Fuller, M. Obrovac, U. von Sacken, Thermal stability of LixCoO2, LixNiO2 and λ-MnO2 and consequences for the safety of Li-ion cells, Solid State ion. 69 (1994) 265–270. http://dx.doi.org/10.1016/0167-2738(94)90415-4.
[5] G. Xu, B. Ding, J. Pan, P. Nie, L. Shen, X. Zhang, High performance lithium–sulfur batteries: advances and challenges, J. Mater. Chem. A. 2 (2014) 12662–12676. http://dx.doi.org/10.1039/C4TA02097A.
[6] R. Xu, J. Lu, K. Amine, Progress in mechanistic understanding and characterization techniques of Li-S batteries, Adv. Energy Mater. 5 (2015) 1–22. http://dx.doi.org/10.1002/aenm.201500408.
[7] Y.X. Yin, S. Xin, Y.G. Guo, L.J. Wan, Lithium-sulfur batteries: electrochemistry, materials, and prospects, Angew. Chem. - Int. Ed. 52 (2013) 13186–13200. http://dx.doi.org/10.1002/anie.201304762.
[8] A.K. Geim, K.S. Novoselov, The rise of graphene, Nat. Mater. 6 (2007) 183–191. http://dx.doi.org/10.1038/nmat1849.
[9] S.H. Chung, R. Singhal, V. Kalra, A. Manthiram, Porous carbon mat as an electrochemical testing platform for investigating the polysulfide retention of various cathode configurations in Li-S cells, J. Phys. Chem. Lett. 6 (2015) 2163–2169. http://dx.doi.org/10.1021/acs.jpclett.5b00927.
[10] S.P. Jand, Y. Chen, P. Kaghazchi, Comparative theoretical study of adsorption of lithium polysulfides (Li2Sx) on pristine and defective graphene, J. Power Sources 308 (2016) 166–171. http://dx.doi.org/10.1016/j.jpowsour.2016.01.062.
[11] F. Li, Y. Su, J. Zhao, Shuttle inhibition by chemical adsorption of lithium polysulfides in B and N co-doped graphene for Li–S batteries, Phys. Chem. Chem. Phys. 18 (2016) 25241–25248. http://dx.doi.org/10.1039/C6CP04071C.
[12] L. Ji, M. Rao, H. Zheng, L. Zhang, Y. Li, W. Duan, J. Guo, E.J. Cairns, Y. Zhang, Graphene oxide as a sulfur immobilizer in high performance lithium/sulfur cells, J. Am. Chem. Soc. 133 (2011) 18522–18525. http://dx.doi.org/10.1021/ja206955k.
[13] Y. Zhong, K.R. Yang, W. Liu, P. He, V. Batista, H. Wang, Mechanistic insights into surface chemical interactions between lithium polysulfides and transition metal oxides, J. Phys. Chem. C. 121 (2017) 14222–14227. http://dx.doi.org/10.1021/acs.jpcc.7b04170.
[14] Z.W. Seh, J.H. Yu, W. Li, P.-C. Hsu, H. Wang, Y. Sun, H. Yao, Q. Zhang, Y. Cui, Two-dimensional layered transition metal disulphides for effective encapsulation of high-capacity lithium sulphide cathodes, Nat. Commun. 5 (2014) 5017. http://dx.doi.org/10.1038/ncomms6017.
[15] Q. Zhang, Y. Wang, Z.W. Seh, Z. Fu, R. Zhang, Y. Cui, Understanding the anchoring effect of two-dimensional layered materials for lithium-sulfur batteries, Nano Lett. 15 (2015) 3780–3786. http://dx.doi.org/10.1021/acs.nanolett.5b00367.
[16] J. Zhao, Y. Yang, R.S. Katiyar, Z. Chen, Phosphorene as a promising anchoring material for lithium–sulfur batteries: a computational study, J. Mater. Chem. A. 4 (2016) 6124–6130. http://dx.doi.org/10.1039/C6TA00871B.
[17] L. Li, L. Chen, S. Mukherjee, J. Gao, H. Sun, Z. Liu, X. Ma, T. Gupta, C.V. Singh, W. Ren, H.M. Cheng, N. Koratkar, Phosphorene as a polysulfide immobilizer and catalyst in high-performance lithium–sulfur batteries, Adv. Mater. 29 (2017) 1–8. http://dx.doi.org/10.1002/adma.201602734.
[18] X. Zhang, J. Hu, Y. Cheng, H.Y. Yang, Y. Yao, S.A. Yang, Borophene as an extremely high capacity electrode material for Li-ion and Na-ion batteries, Nanoscale 8 (2016) 15340–15347. http://dx.doi.org/10.1039/C6NR04186H.
[19] L. Shi, T. Zhao, A. Xu, J. Xu, Ab initio prediction of borophene as an extraordinary anode material exhibiting ultrafast directional sodium diffusion for sodium-based batteries, Sci. Bull. 61 (2016) 1138–1144. http://dx.doi.org/10.1007/s11434-016-1118-7.
[20] B. Mortazavi, A. Dianat, O. Rahaman, G. Cuniberti, T. Rabczuk, Borophene as an anode material for Ca, Mg, Na or Li ion storage: a first-principle study, J. Power Sources 329 (2016) 456–461. http://dx.doi.org/10.1016/j.jpowsour.2016.08.109.
[21] C. Cheng, J.-T. Sun, H. Liu, H.-X. Fu, J. Zhang, X.-R. Chen, S. Meng, Suppressed superconductivity in substrate-supported β_{12} borophene by tensile strain and electron doping, 2D Mater. 4 (2017) 25032. http://dx.doi.org/10.1088/2053-1583/aa5e1b.
[22] B. Peng, H. Zhang, H. Shao, Y. Xu, R. Zhang, H. Zhu, Electronic, optical, and thermodynamic properties of borophene from first-principle calculations, J. Mater. Chem. C 4 (2016) 3592–3598. http://dx.doi.org/10.1039/C6TC00115G.
[23] B. Mortazavi, O. Rahaman, A. Dianat, T. Rabczuk, Mechanical responses of borophene sheets: a first-principles study, Phys. Chem. Chem. Phys. 18 (2016) 27405–27413. http://dx.doi.org/10.1039/C6CP03828J.
[24] M.Q. Le, B. Mortazavi, T. Rabczuk, Mechanical properties of borophene films: a reactive molecular dynamics investigation, Nanotechnology. 27 (2016) 445709. http://dx.doi.org/10.1088/0957-4484/27/44/445709.
[25] A.R. Oganov, J. Chen, C. Gatti, Y. Ma, Y. Ma, C.W. Glass, Z. Liu, T. Yu, O.O. Kurakevych, V.L. Solozhenko, Ionic high-pressure form of elemental boron, Nature. 457 (2009) 863–867. http://dx.doi.org/10.1038/nature07736.
[26] Y. Liu, E.S. Penev, B.I. Yakobson, Probing the synthesis of two-dimensional boron by first-principles computations, Angew. Chem. - Int. Ed. 52 (2013) 3156–3159. http://dx.doi.org/10.1002/anie.201207972.
[27] S. Xu, Y. Zhao, J. Liao, X. Yang, H. Xu, The formation of boron sheet at the Ag (111) surface : From clusters , ribbons , to monolayers, 2016.
[28] A.J. Mannix, X.-F. Zhou, B. Kiraly, J.D. Wood, D. Alducin, B.D. Myers, X. Liu, B.L. Fisher, U. Santiago, J.R. Guest, M.J. Yacaman, A. Ponce, A.R. Oganov, M.C. Hersam, N.P. Guisinger, Synthesis of borophenes: anisotropic, two-dimensional boron polymorphs, Science 80 (350) (2015) 1513–1516. http://dx.doi.org/10.1126/science.aad1080.
[29] B. Feng, J. Zhang, Q. Zhong, W. Li, S. Li, H. Li, P. Cheng, S. Meng, L. Chen, K. Wu, Experimental realization of two-dimensional boron sheets, Nat. Chem. 8 (2016) 563–568. http://dx.doi.org/10.1038/nchem.2491.
[30] [30] P. Giannozzi, S. Baroni, N. Bonini, M. Calandra, R. Car, C. Cavazzoni, D. Ceresoli, G.L. Chiarotti, m. Cococcioni, I. Dabo, A.D. Corso, S. Fabris, G. Fratesi, S. de Gironcoli, R. Gebauer, U. Gerstmann, C. Gougoussis, A. Kokalj, M. Lazzeri, L. Martin-Samos, N. Marzari, F. Mauri, R. Mazzarello, S. Paolini, A. Pasquarello, L. Paulatto, C. Sbraccia, S. Scandolo, G. Sclauzero, A.P. Seitsonen, A. Smogunov, P. Umari, R.M. Wentzcovitch, Quantum ESPRESSO: a modular and open-source software project for quantum simulations of materials, 2009. doi:10.1088/0953-8984/21/39/395502.
[31] J.P. Perdew, K. Burke, M. Ernzerhof, Generalized gradient approximation made simple, Phys. Rev. Lett. 77 (1996) 3865–3868. http://dx.doi.org/10.1103/PhysRevLett.77.3865.
[32] J.D. Pack, H.J. Monkhorst, "special points for Brillouin-zone integrations"-a reply, Phys. Rev. B. 16 (1977) 1748–1749. http://dx.doi.org/10.1103/PhysRevB.16.1748.
[33] V. Barone, M. Casarin, D. Forrer, M. Pavone, M. Sambi, A. Vittadini, Role and effective treatment of dispersive forces in materials: polyethylene and graphite crystals as test cases, J. Comput. Chem. 30 (2009) 934–939. http://dx.doi.org/10.1002/jcc.21112.
[34] G. Henkelman, B.P. Uberuaga, H. Jónsson, Climbing image nudged elastic band method for finding saddle points and minimum energy paths, J. Chem. Phys. 113 (2000) 9901–9904. http://dx.doi.org/10.1063/1.1329672.
[35] J. Gao, L. Li, J. Tan, H. Sun, B. Li, J.C. Idrobo, C.V. Singh, T.M. Lu, N. Koratkar, Vertically oriented arrays of ReS2 nanosheets for electrochemical energy storage and electrocatalysis, Nano Lett. 16 (2016) 3780–3787. http://dx.doi.org/10.1021/acs.nanolett.6b01180.
[36] M. Safari, C.Y. Kwok, L.F. Nazar, Transport properties of polysulfide species in lithium-sulfur battery electrolytes: coupling of experiment and theory, ACS Cent. Sci. 2 (2016) 560–568. http://dx.doi.org/10.1021/acscentsci.6b00169.
[37] M. Cuisinier, P.E. Cabelguen, S. Evers, G. He, M. Kolbeck, A. Garsuch, T. Bolin, M. Balasubramanian, L.F. Nazar, Sulfur speciation in Li-S batteries determined by operando X-ray absorption spectroscopy, J. Phys. Chem. Lett. 4 (2013) 3227–3232. http://dx.doi.org/10.1021/jz401763d.
[38] M. Wild, L. O'Neill, T. Zhang, R. Purkayastha, G. Minton, M. Marinescu, G.J. Offer, Lithium sulfur batteries, a mechanistic review, Energy Environ. Sci. 8 (2015) 3477–3494. http://dx.doi.org/10.1039/C5EE01388G.
[39] T. Zhou, W. Lv, J. Li, G. Zhou, Y. Zhao, S. Fan, B. Liu, B. Li, F. Kang, Q.-H. Yang, Twinborn TiO_2 –TiN heterostructures enabling smooth trapping–diffusion–conversion of polysulfides towards ultralong life lithium–sulfur batteries, Energy Environ. Sci. 10 (2017) 1694–1703. http://dx.doi.org/10.1039/C7EE01430A.
[40] G. Zhou, E. Paek, G.S. Hwang, A. Manthiram, High-performance lithium-sulfur batteries with a self-supported, 3D Li2S-doped graphene aerogel cathodes, Adv. Energy Mater. 6 (2016) 1–9. http://dx.doi.org/10.1002/aenm.201501355.
[41] D. Rao, L. Zhang, Y. Wang, Z. Meng, X. Qian, J. Liu, X. Shen, G. Qiao, R. Lu, Mechanism on the Improved Performance of Lithium Sulfur Batteries with MXene-Based Additives, J. Phys. Chem. C 121 (2017) 11047–11054. http://dx.doi.org/10.1021/acs.jpcc.7b00492.
[42] G. Zhou, E. Paek, G.S. Hwang, A. Manthiram, High-performance lithium-sulfur batteries with a self-supported, 3D Li2S-doped graphene aerogel cathodes, Adv. Energy Mater. 6 (2016) 1–9. http://dx.doi.org/10.1002/aenm.201501355.
[43] X. Chen, H.-J. Peng, R. Zhang, T.-Z. Hou, J.-Q. Huang, B. Li, Q. Zhang, An

analogous periodic law for strong anchoring of polysulfides on polar hosts in lithium sulfur batteries: S- or Li-binding on first-row transition-metal sulfides?, ACS Energy Lett. 2 (2017) 795–801. http://dx.doi.org/10.1021/acsenergylett.7b00164.

[44] G. Zhou, H. Tian, Y. Jin, X. Tao, B. Liu, R. Zhang, Z.W. Seh, D. Zhuo, Y. Liu, J. Sun, J. Zhao, C. Zu, D.S. Wu, Q. Zhang, Y. Cui, Catalytic oxidation of Li $_2$ S on the surface of metal sulfides for Li–S batteries, Proc. Natl. Acad. Sci. 114 (2017) 840–845. http://dx.doi.org/10.1073/pnas.1615837114.

[45] T.Z. Hou, X. Chen, H.J. Peng, J.Q. Huang, B.Q. Li, Q. Zhang, B. Li, Design principles for heteroatom-doped nanocarbon to achieve strong anchoring of polysulfides for lithium–sulfur batteries, Small. C (2016) 3283–3291. http://dx.doi.org/10.1002/smll.201600809.

[46] G. Tan, R. Xu, Z. Xing, Y. Yuan, J. Lu, J. Wen, C. Liu, L. Ma, C. Zhan, Q. Liu, T. Wu, Z. Jian, R. Shahbazian-Yassar, Y. Ren, D.J. Miller, L.A. Curtiss, X. Ji, K. Amine, Burning lithium in CS2 for high-performing compact Li2S–graphene nanocapsules for Li–S batteries, Nat. Energy. 2 (2017) 17090. http://dx.doi.org/10.1038/nenergy.2017.90.

[47] X. Liang, A. Garsuch, L.F. Nazar, Sulfur cathodes based on conductive MXene nanosheets for high-performance lithium-sulfur batteries, Angew. Chem. - Int. Ed. 54 (2015) 3907–3911. http://dx.doi.org/10.1002/anie.201410174.